Please cite the Published Version

Additional Information: This is an Open Access article which appeared in Dental Materials, published by Elsevier

Effect of surface treatments on optical, topographical and mechanical properties of CAD/CAM reinforced lithium silicate glass ceramics

Hanan Al-Johani[a,b], Julfikar Haider[a,c], Nick Silikas[a,*], Julian Satterthwaite[a]

[a] *Division of Dentistry, School of Medical Sciences, University of Manchester, UK*
[b] *Department of Restorative Dentistry, Division of Biomaterials, Faculty of Dentistry, King Abdulaziz University, Saudi Arabia*
[c] *Department of Engineering, Manchester Metropolitan University, Manchester, United Kingdom*

ABSTRACT

Objectives: To investigate the effect of different surface treatments on optical, topographical and mechanical properties of CAD/CAM lithium silicate-based glass ceramics (LSC's) and their combined effect on the output of a light curing unit (LCU).
Methods: Four CAD/CAM LSC's were investigated: Lithium Disilicate (Emax CAD; EC), Zirconia-reinforced silicates (Vita Suprinity; VS and Celtra Duo;CD) and Lithium Aluminum Disilicate (CEREC Tessera; CT). Ceramic specimens (n = 240) were divided into six subgroups according to their surface treatment: (a) Control, (b) Hydrofluoric acid (HF) 5%, (c) HF 5% + Neutralizing agent (N), (d) HF 9%, (e) HF 9% +N and (f) Self-etching ceramic primer (SEP). Irradiance, power and radiant exposure of a LCU were measured with MARC-LC following ceramic specimen interposition. Direct light transmission (T%) and absorbance (Abs%) of the specimens were measured with UV-Vis spectrophotometry. Roughness (Sa, Sq) and wettability (θ°) were measured with optical profilometry and sessile drop profile analysis, respectively. Biaxial flexural strength (σ) of the ceramic specimens was measured by the ball-on-three-balls method and ceramic specimens were examined microscopically. Statistical analyses was performed by two-way ANOVA followed by post hoc multiple comparisons (α = 0.05).
Results: Acid neutralization decreased T% and increased Abs% in all LSC's and highest T% was exhibited with VS. Neutralized EC, VS and CD displayed higher Sa in HF9, while neutralized CT displayed higher Sa in HF5. Self-etch primer significantly reduced θ° (p < 0.001). σ was observed in the followed ascending order: HF9 +N < HF9 < HF5 +N < HF5 < SEP < Control for all LSC's.
Significance: Optical, topographical and mechanical properties of the CAD/CAM ceramic blocks were strongly dependent on the type of surface treatment. Results of neutralization post-etching indicate promising potential for future investigations.

1. Introduction

In the last two decades, lithium silicate-based glass ceramics (LSC's) have become increasingly popular as dental restorative materials due to their optimally combined aesthetics and mechanical properties as well as their wide range of clinical indications [1]. Computer-aided design/computer-assisted manufacturing (CAD/CAM) technology has created a paradigm shift in the development of LSC's with an array of compositions that have been emerging in the market at an advanced rate [2]. Introduced in 2005, IPS e.max CAD, Ivoclar Vivadent, Schaan, Liechtenstein) is a machinable LSC with established long-term clinical survival [3,4]. However, in attempt to improve mechanical performance, other manufacturers have recently introduced LSC's reinforced with 10 wt%

zirconia in their glassy matrix (Celtra Duo, Dentsply Sirona, York, PA, USA; VITA Suprinity, VITA Zahnfabrik, Bad Säckingen, Germany). The most recent LSC added to the market is commercially marketed as an Advanced Lithium Disilicate glass ceramic (CEREC Tessera, Dentsply Sirona, York, PA, USA), which contains lithium aluminium disilicate crystals known as virgilite within its glassy zirconia matrix [5]. While some machinable LSC's are found in a pre-crystallized condition to ensure rapid milling, others are provided in a fully-crystallized state to minimize post-milling heat treatment and provide patients with a faster turnaround time when single visit restorations are indicated [2, 6, 7].

In order to establish an optimum long-term bond between ceramic restorations and tooth substrate, different surface treatment regimens have been employed to prepare the internal surfaces of LSC. Alteration

of the intaglio surface of LSC's increases the surface area thus improving the chemical reactivity of the ceramic surface and the micromechanical retention of luting cements. Surface alterations can be accomplished by chemical, mechanical or chemo-mechanical treatments. Mechanical methods include airborne particle abrasion and diamond rotary bur grinding, chemical methods involve etching the ceramics with different acidic agents and chemo-mechanical treatments are accomplished by tribochemical silica-coating [8–11]. Depending on the chemical composition of the ceramic materials, their chemical reactivity to acidic agents differs; ceramics with higher glass content are more acid sensitive, while polycrystalline ceramics are acid resistant [12]. Hydrofluoric acid (HF) is the most utilised acid for treating the internal surfaces of LSC's. HF creates a porous structure by reacting with the silica matrix of the ceramic to form silicon tetrafluoride (SiF_4), which then further reacts to form a fluorosilicic acid that is washed away upon rinsing of the ceramic restoration resulting in exposure of the underlying crystalline structure of LSC's thus creating a porous microstructure [8]. Due to its potential dermal penetration and systemic toxicity, HF must be used extraorally and ultrasonic cleaning of the ceramics restorations is imperative to remove acidic remnants [13]. Nevertheless, evidence of residual HF in ceramic surfaces post-rinsing has been confirmed by microscopic imaging [14,15]. Therefore, to minimize any potential side-effects, alternative etching regimens have been proposed. Neutralizing agents can be applied to ceramic surfaces post-etching to neutralize the acidic pH of HF and render it less hazardous as the products of the acid–base reaction are insoluble fluoride salts [16–18]. The application of a neutralizing agent on etched ceramic surfaces has been reported to arrest the action of HF and prevent further topographical alterations [19–21]. Self-etch ceramic primers (SEP) have also been recommended as a less toxic substitute to HF and are capable of both etching and priming without the need for separate HF etching and silane coating steps [22,23].

Topographical maps of ceramic surfaces post-treatment provide several surface texture parameters that can exemplify the extent of volumetric loss caused by the acidic action of HF [24]. Wettability assessment by means of contact angle measurements can aid in determining the degree of hydrophilicity of ceramic surfaces and thereby inferring the bonding performance of luting cements [25,26]. Photometric characteristics of a ceramic restoration are affected by changes in their surface texture, thickness and chemical composition. Light attenuation through ceramic restorations may weaken bond strengths to photopolymerized resin cement lutes thus reducing the restoration longevity [27,28]. Due to the fixed geometry of CAD/CAM blocks, specimen preparation for standardized uniaxial and biaxial flexural strength test methods is difficult to accomplish. The ball-on-three-balls (B3B) biaxial strength test method was developed by Börger et al. [29] specifically for ceramic materials. The B3B method facilitates testing rectangular ceramic plates with deviation in flatness up to 16%. The unique set-up of stainless steel balls in B3B reduces any friction interferences and generates a stress field at the tensile side of the ceramic with a three-fold symmetry providing an accurate clinical simulation [29–31].

Although neutralization is considered an effective pre-bonding step to enhance the longevity of dental ceramic restorations [16,32], its effect in terms of altering the optical, topographical and mechanical properties of reinforced lithium silicate ceramics has not been fully investigated. Therefore, the aim of this study was to investigate the effect of different surface treatment protocols on the optical (light transmission, and absorption), topographical (roughness and wettability) and mechanical properties (biaxial flexural strength) of four CAD/CAM lithium silicate-based ceramics and their effects on the light output of a light curing unit.

The following null hypotheses were formulated:

1. There is no effect on the output of a light curing unit following interposition of CAD/CAM lithium silicate-based ceramics exposed to different chemical surface treatments.

2. Different chemical surface treatments do not have any effect on the optical, topographical or mechanical properties of CAD/CAM lithium silicate-based ceramics.

2. Materials and methods

2.1. Specimen preparation

Four CAD/CAM glass ceramics were tested: lithium disilicate (EC: e.max CAD), two zirconia-reinforced lithium silicates (VS: Vita Suprinity and CD: Celtra Duo), and lithium aluminium disilicate (CT: CEREC Tessera). Ceramic blocks were sectioned using a precision cutting machine (IsoMet 1000 Buehler, Germany) then sintered in a furnace (Programat EP5000, Ivoclar Vivadent) based on manufacturers' recommended firing schedules. Subsequently, specimens were polished following a polishing sequence of 400, 800, 1000 and 1200-grit silicon carbide papers at 350 rpm under running water in a mechanical grinding device (Metaserv 250, Buehler, Germany). The final dimension of the specimens was $12 \times 12 \times 1.5$ mm^3 ($\pm$ 0.05 mm). All specimens (n = 240) were divided into 6 subgroups (n = 10) for each material according to their surface treatment protocol; Group 1: Control, Group 2: HF 5%, Group 3: HF 5% + Neutralizing agent, Group 4: HF 9%, Group 5: HF 9% + Neutralizing agent, Group 6: Self-etch primer. The neutralizing solution was prepared by dissolving 50 g of calcium carbonate and sodium bicarbonate powder (IPS Neutralizing Powder, Ivoclar Vivadent) in 250 ml of water [33]. During their immersion in the neutralizing solution, specimens were placed in a stainless steel mesh for ease of retrieval from the opaque solution after the allotted treatment time. All materials and surface treatments included in the study are described in Tables 1 and 2, respectively.

2.2. Photometric properties

2.2.1. Light curing unit characterisation

The power (mW), irradiance (mW/cm^2) and radiant exposure (J/cm^2) of the LCU was measured by a Managing Accurate Resin Curing-Light Collector (MARC-LC, BlueLight analytics Inc, Halifax, Canada) spectrophotometer equipped with analytical software and a light emitting diode LCU (Elipar S10, 3 M ESPE, St. Paul, MN, USA). A customized mould was utilized to centre the ceramic specimens on the bottom sensor of MARC-LC with the treated surface facing away from the light curing tip. The position of the LCU was fixed with a mechanical arm to establish a zero distance between the LCU tip and the specimens. The LCU was fully charged prior to any measurements with a wavelength ranging between 430 and 480 nm and mean irradiance and power of 1600 mW/cm^2 and 200 mW, respectively. Power loss (%) of the LCU was calculated as the percentage of decrease obtained by Eq. [1]:

$$\text{Power loss}(\%) = \left(\frac{Power_{WO} - Power_{W}}{Power_{WO}} \right) *100 \tag{1}$$

Where subscripts *wo* and *w* refer to LCU measurements *without* and *with* an interposing ceramic specimen respectively. Similarly, loss in irradiance and radiant exposure were calculated as percentages of decrease in each property. Five specimens of each subgroup were measured twice (n = 120, 10 measurements per subgroup) during a 20 s light exposure cycle in the continuous mode setting.

2.2.2. Light transmittance measurements

A quantitative measurement of the translucency of the ceramic specimens was acquired by measuring the direct transmission of light through the specimens (excluding scattered or reflected light beams). Direct light transmittance (T%) was calculated by Eq. [2]:

$$T\% = \frac{I_t}{I_0} \tag{2}$$

Table 1
Experimental materials and manufacturers' information.

Materials	Brand	Manufacturer	Chemical Composition (wt%)
Lithium Disilicate	e.max CAD (EC)	Ivoclar Vivadent (Liechtenstein)	57–80% SiO_2, 11–19% LiO_2, 0–13% K_2O, 0% − 11% P_2O_5, 0–8% ZrO_2, 0–8% ZnO, 0–5% Al_2O_3, 0–5% MgO
Zirconia- reinforced Lithium Silicate	Vita Suprintiy (VS)	Vita-Zahnfabrik (Germany)	56–64% SiO_2, 15–21% Li_2O, 8–12% ZrO_2, 3–8% P_2O_5, 1–4% Al_2O_3, 1–4% K_2O, 0–4% CeO_2, 0.1% La_2O_3, 0–6% pigments
Zirconia-reinforced Lithium Silicate	Celtra Duo (CD)	Dentsply Sirona (USA)	58% SiO_2, 18.5% Li_2O, 10.1% ZrO_2, 5% P_2O_5, 1.9% Al_2O_3, 2%CeO_2, 1% Tb_4O_7
Lithium Aluminium Disilicate	CEREC Tessera (CT)	Dentsply Sirona (USA)	90% $Li_2Si_2O_5$, 5% Li_3PO_4, 5% $Li_{0.5}Al_{0.5}Si_{2.5}O_6$
Hydrofluoric Acid	IPS Ceramic Etching Gel	Ivoclar Vivadent (Liechtenstein)	5% buffered hydrofluoric acid
Hydrofluoric Acid	Porcelain Etch 9.5%	Ultradent (USA)	9.5% buffered hydrofluoric acid
Neutralizing Agent	IPS Neutralizing Powder	Ivoclar Vivadent (Liechtenstein)	Calcium carbonate and sodium bicarbonate
Self-etching Primer	Monobond Etch & Prime	Ivoclar Vivadent (Liechtenstein)	Butanol, trimethoxypropyl methaycrylate, tetrabutylammonium dihydrogen trifluoride, methacrylated phosphoric acid ester, colorant
Silane Primer	Monobond Plus	Ivoclar Vivadent (Liechtenstein)	Silane methacrylate, phosphoric acid methacrylate, ethanol and sulfide methacrylate

Where I_t is the transmitted light beam intensity and I_0 is the incident light beam intensity.

T% of the ceramic specimens was measured with a double beam UV-Vis spectrophotometer (Cary 60 UV-Vis Spectrophotometer, Agilent Technologies, Santa Clara, CA, USA) in the transmittance mode at wavelengths ranging between 350 nm and 800 nm with 600 nm/min scanning rate and 1 nm data interval. Baseline correction was performed to balance the reference and sample beams in the absence of a specimen. Afterwards, the specimen was placed in a solid sample holder with the treated surface facing away from the light source. The dual beam mode of the spectrophotometer allowed calculation of both incident and transmitted light simultaneously. Abs% of the ceramic specimens was measured by the UV-Vis spectrophotometer in the absorbance mode using the same wavelength range and scanning parameters previously described. Five specimens of each subgroup (n = 120) were investigated and comparisons of mean T% and Abs% values were done at 525 nm wavelength which represents the midpoint of visible light wavelength spectrum [34,35].

2.3. Topographical properties

2.3.1. Roughness

The treated surfaces of five randomly selected specimens from each subgroup were scanned with a non-contact optical profilometer equipped with 400 μm chromatic length aberration (Talysurf CLI 1000, Taylor Hobson Precision, Leicester, UK). Measurements were taken in a horizontal bidirectional method with a resolution of 501 points, at a 500 μm/s scanning rate and a 5 μm spacing between the measurement points on both x- and y- axes. A Gaussian regression filter was applied with a cut-off wavelength value of 0.25 μm. Three-dimensional topographical maps were obtained and roughness was reported in terms of roughness parameters Sa and Sq (μm) in accordance with ISO 25178–2:2012, where Sa is the arithmetic mean height deviation within

the sample surface area and Sq is the root mean square height deviation within the sample surface area. The scanned surface area was 2.5×2.5 mm^2 and six measurements were acquired per specimen (n = 120, 30 measurements per subgroup).

2.3.2. Wettability

Wettability of the treated surfaces was determined by calculating the Young contact angle (θ°) in the static mode by sessile drop profile analysis using a Drop Shape Analyzer (DSA100, KRUSS). A droplet of 1 μl of silane primer (Monobond Plus, Ivoclar Vivadent) was deposited by a syringe positioned above the sample surface, and a high-resolution camera captured the image from the profile view precisely 10 s after depositing the drop. The image was analysed using image analysis software to trace the droplet arc and to determine the tangent value on left and right side of each drop. The mean contact angle was then calculated from the contact angles measured on both sides of the drop. Five specimens from each subgroup were examined and 2 drops were measured per specimen (n = 120, 10 measurements per subgroup). Upon calculating the contact angles, the treated surfaces were classified as superhydrophilic (θ° ≈ 0°), hydrophilic (0° < θ° < 90°), hydrophobic (θ° > 90°), or superhydrophobic (θ° > 150°) [36].

2.3.3. Surface microscopy

A field emission scanning electron microscope (FE-SEM) (Supra 40 VP, Carl Zeiss Ltd, Cambridge, UK) was employed to observe the microstructure and topography of a randomly-assigned specimen of EC, VS, CD and CT from each treatment group. Prior to imaging, specimens were cleaned with ethanol for 1 min and then left to dry for 24 h at room temperature. Images of the ceramic crystalline microstructure were obtained at 20,000x magnification and an accelerating voltage of 20 kV.

Table 2
Experimental surface treatments.

Group	Surface treatment protocols
Control	No surface treatment
HF5	Etched with HF 5% for 30 s, rinsed under running water for 1 min followed by an ultrasonic cleaning for 5 min
HF5 +N	Etched with HF 5% for 30 s, rinsed under running water for 1 min, placed in a neutralizing solution for 1 min followed by an ultrasonic cleaning for 5 min
HF9	Etched with HF 9% for 30 s, rinsed under running water for 1 min followed by an ultrasonic cleaning for 5 min
HF9 +N	Etched with HF 9% for 30 s, rinsed under running water for 1 min, placed in a neutralizing solution for 1 min followed by an ultrasonic cleaning for 5 min
SEP	Etched with a self-etch primer, 20 s active application with microbrush, then 40 s passive application, rinsed under running water for 1 min followed by an ultrasonic cleaning for 5 min

2.4. Biaxial flexural strength

The ball-on-three balls (B3B) set-up was used to measure the flexural strength of the specimens in a universal testing machine (Zwick/Roell Z020, Zwick, Ulm, Germany). The ceramic specimens (n = 240) were positioned between three loading balls and a single support ball on the compressive and tensile sides, respectively with the treated surfaces of the specimens facing toward the tensile side. The sequence of operation in B3B tests is shown in Fig. 1 and Fig. S1. All stainless-steel balls had equal radii (R_b = 4 mm) and a preload of 10 N was applied prior to removal of the positioning guide to permit the support balls to roll freely as fracture of the ceramic specimens ensued. A compressive load was applied with a 20 kN load cell at 0.5 mm/min crosshead speed and the flexural strength (σ) was recorded as the maximum stress created on the tensile side of the specimen at fracture and was calculated by Eq. [3]:

$$\sigma = \delta \quad F_{\max}/t^2 \tag{3}$$

Where t is the thickness of the specimen, F_{max} is the force at fracture, and δ is a function determined by three independent variables [31]: the dimensional ratio formed by the support radius R_a (R_a = $(2\sqrt{3}R_b)/3$) and the radius of the specimen R, (R_a/R), the thickness to specimen radius ratio (t/R) and the Poisson's ratio of the tested material (v). δ can be calculated using Eq. [4]:

$$
\begin{aligned}
\delta &= 0.323308 \\
&+ \frac{\left[\left[(1.30843 + 1.44301v)\right]\left[1.78428 - 3.15347\left(\frac{t}{R_a}\right) + 6.67919\left(\frac{t}{R_a}\right)^2 - 4.62603\left(\frac{t}{R_a}\right)^3\right]\right]}{\left[1 + 1.71955\left(\frac{t}{R_a}\right)\right]}
\end{aligned}
\tag{4}
$$

Poisson ratios for EC, VS, CD and CT were 0.216, 0.208, 0.22 and 0.229 respectively [2].

Weibull analysis was conducted to determine the reliability in the flexural strength of the ceramic specimens following the surface treatment using the flexural strength values obtained from B3B strength testing. The Weibull modulus (m) was calculated using Eq. [5]:

$$P_f(\sigma) = 1 - \exp\left[-\left(\frac{\sigma}{\sigma_0}\right)^m\right] \tag{5}$$

Where $P_f(\sigma)$ is the probability of failure for a given flexural strength, σ is the fracture strength σ_0 is the characteristic strength at the fracture probability of 63.2%, and m is the Weibull modulus. Upper and lower limits of the 95% confidence intervals for σ_0 and m were calculated following DIN ENV 843–5:2007 [37].

2.5. Statistical data analysis

G*power software (V. 3.1.3; Heinrich Hein University, Germany) was used to calculate the sample size needed to achieve 80% power probability, hence 5 specimens/ per subgroup were chosen for roughness, wettability, optical and LCU properties and 10 specimens/ per subgroup were chosen for biaxial flexural strength measurements. Data analysis was performed by statistical software (SPSS 29.0; IBM SPSS Statistics Inc., Chicago, IL, USA). Assumption of normality and homogeneity was confirmed with the Kolmogorov-Smirnov test and Levene's test, respectively. Two-way ANOVA was performed to determine both the effect of factors ceramic type and etching treatment and the interaction of both factors on the measured properties (α ≤ 0.05) and Pearson correlation was used to analyse significant relationships between the different properties. Post hoc Tukey test was performed to detect significant pairwise comparisons within and between different materials and surface treatments (p ≤ 0.05).

3. Results

3.1. Photometric properties

3.1.1. LCU characterisation

Mean power (mW), irradiance (mW/cm²), radiant exposure (J/cm²) are reported in Table 3 and mean percentages of loss relative to each property are presented in Table S1. Results of the two-way ANOVA indicated that the type of ceramic material, surface treatment and the interaction between both the variables were statistically significant ($p < 0.001$) on LCU irradiance and power measurements. The type of ceramic material significantly affected the radiant exposure (J/cm²) of the LCU ($p < 0.001$) however the type of surface treatment did not have a significant effect on the radiant exposure of the LCU ($p = 0.068$). Interposition of the ceramic specimens significantly reduced the LCU's output regardless of the type of ceramic material or the type of surface treatment with loss percentages in power, irradiance and radiant exposure ranging from 57.3% to 84.3%, 60.4–81.9% and 55.6–81.6%, respectively. When comparing different ceramic materials, the LCU displayed highest irradiance, power and radiant exposure when the light was transmitted through the EC specimens in comparison to the other interposing ceramic materials. Significantly higher percentage of loss in LCU irradiance, power and radiant exposure was seen in CT specimens in comparison to other ceramic materials.
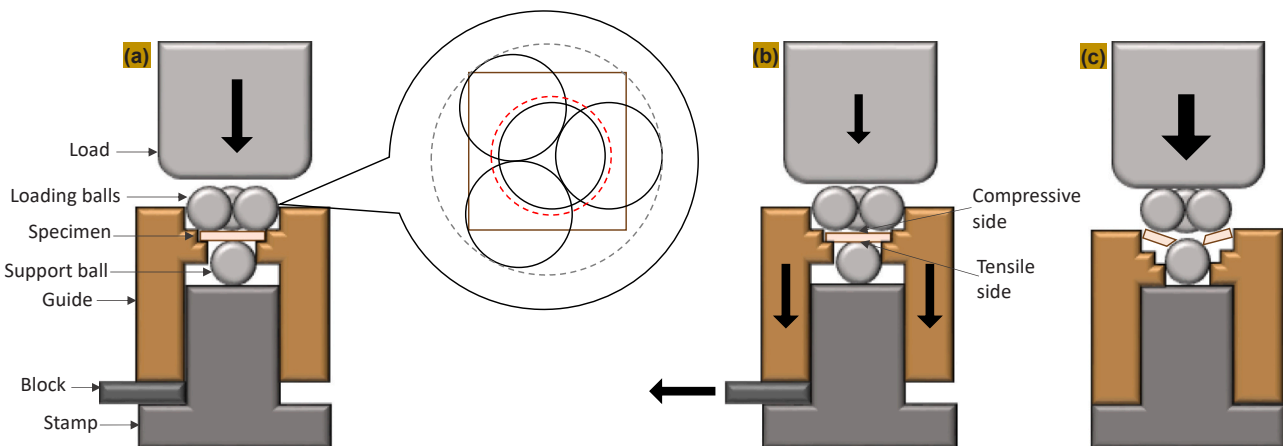

Fig. 1. (a) Schematic representation of B3B flexural strength test; where red dashed line is the support ball radius and the black solid line is the loading ball radius, (b) Preload is applied before removing the block, (c) Compressive load is applied and the flexural strength (σ) is recorded and (d) B3B test apparatus set-up in a universal testing machine.

Table 3

Light curing unit characterisation: Mean power (mW), irradiance (mW/cm^2) and radiant exposure (J/cm^2).

Group	Power (mW) Mean ± SD	Irradiance (mW/cm^2) Mean ± SD	Radiant exposure (J/cm^2) Mean ± SD
EC-Control	85.2 ± 2.8^{A1}	604.0 ± 10.8^{B1}	11.8 ± 0.6^{B1}
EC-HF5	80.0 ± 1.5^{B1}	587.6 ± 15.5^{B1}	11.7 ± 0.5^{B1}
EC-HF5 + N	78.4 ± 2.7^{B1}	577.2 ± 7.4^{B1}	11.8 ± 0.5^{B1}
EC-HF9	82.2 ± 2.5^{AB1}	593.2 ± 16.5^{B1}	12.6 ± 0.5^{AB1}
EC-HF9 + N	81.0 ± 1.5^{AB1}	587.6 ± 11.3^{B1}	12.3 ± 0.3^{AB1}
EC-SEP	85.4 ± 2.8^{A1}	634.4 ± 23.7^{A1}	13.3 ± 1.1^{A1}
VS-Control	69.8 ± 4.5^{A2}	482.4 ± 12.8^{A3}	11.5 ± 0.9^{A1}
VS-HF5	63.7 ± 4.1^{AB2}	466.4 ± 14.8^{A2}	11.3 ± 0.1^{A1}
VS-HF5 + N	62.3 ± 3.3^{B3}	459.4 ± 6.1^{AB3}	11.3 ± 0.2^{A2}
VS-HF9	68.4 ± 3.1^{AB2}	484.4 ± 23.3^{A3}	11.4 ± 0.3^{A2}
VS-HF9 + N	62.8 ± 2.2^{B3}	435.0 ± 15.0^{B3}	10.9 ± 0.2^{A2}
VS-SEP	67.6 ± 0.6^{AB3}	486.6 ± 1.9^{A3}	11.2 ± 0.1^{A2}
CD-Control	74.4 ± 0.9^{AB2}	565.4 ± 33.9^{A2}	11.8 ± 0.1^{A1}
CD-HF5	74.8 ± 2.9^{A1}	549.6 ± 14.5^{B1}	11.7 ± 0.2^{A1}
CD-HF5 + N	68.8 ± 2.6^{C2}	493.0 ± 24.2^{C2}	11.1 ± 0.1^{B2}
CD-HF9	71.4 ± 0.6^{BC2}	516.8 ± 4.6^{BC2}	11.2 ± 0.1^{B2}
CD-HF9 + N	72.0 ± 0.7^{ABC2}	523.4 ± 5.1^{BC2}	11.2 ± 0.1^{B2}
CD-SEP	73.2 ± 0.8^{AB2}	539.6 ± 7.6^{AB2}	11.3 ± 0.0^{B2}
CT-Control	37.4 ± 3.7^{AB3}	350.8 ± 16.2^{A4}	6.1 ± 0.6^{A2}
CT-HF5	31.4 ± 4.4^{B3}	329.6 ± 33.6^{B3}	6.0 ± 0.6^{A2}
CT-HF5 + N	41.6 ± 2.9^{A4}	305.0 ± 11.8^{B4}	5.9 ± 0.2^{A3}
CT-HF9	41.2 ± 2.6^{A3}	321.0 ± 3.16^{AB4}	6.4 ± 0.4^{A3}
CT-HF9 + N	38.6 ± 3.5^{AB4}	290.4 ± 18.1^{B4}	5.7 ± 0.5^{A3}
CT-SEP	40.0 ± 5.2^{A4}	325.4 ± 28.2^{AB4}	5.5 ± 0.3^{A3}

Note: Different superscript letters indicate significant statistical differences between the surface treatments within same material, different superscript numbers indicate significant statistical differences between materials within the same surface treatment (p ≤ 0.05).

Table 4

Direct light transmittance (T%) and absorbance (Abs%) values of CAD/CAM lithium silicate-based ceramics at 525 nm wavelength.

Group	T% Mean ± SD	Abs% Mean ± SD
EC-Control	0.5 ± 0.02^{A2}	2.3 ± 0.04^{C1}
EC-HF5	0.3 ± 0.03^{C2}	2.6 ± 0.09^{B1}
EC-HF5 + N	0.1 ± 0.02^{D4}	2.2 ± 0.04^{C3}
EC-HF9	0.4 ± 0.02^{C3}	2.8 ± 0.04^{A1}
EC-HF9 + N	0.3 ± 0.04^{C2}	2.5 ± 0.06^{B2}
EC-SEP	0.4 ± 0.02^{B2}	2.3 ± 0.04^{C1}
VS-Control	1.7 ± 0.04^{A1}	2.1 ± 0.06^{C2}
VS-HF5	0.7 ± 0.07^{D1}	2.4 ± 0.03^{A2}
VS-HF5 + N	0.4 ± 0.03^{E1}	2.3 ± 0.04^{B3}
VS-HF9	0.8 ± 0.02^{C1}	2.1 ± 0.04^{C4}
VS-HF9 + N	0.7 ± 0.05^{D1}	2.2 ± 0.06^{C3}
VS-SEP	1.2 ± 0.02^{B1}	1.7 ± 0.04^{D2}
CD-Control	0.5 ± 0.15^{A2}	2.3 ± 0.15^{D1}
CD-HF5	0.3 ± 0.02^{B2}	2.7 ± 0.04^{A1}
CD-HF5 + N	0.8 ± 0.04^{B3}	2.6 ± 0.07^{AB1}
CD-HF9	0.3 ± 0.01^{B3}	2.6 ± 0.03^{ABC2}
CD-HF9 + N	0.3 ± 0.03^{B2}	2.5 ± 0.02^{BC2}
CD-SEP	0.4 ± 0.07^{AB23}	2.4 ± 0.11^{CD1}
CT-Control	0.4 ± 0.03^{A2}	2.2 ± 0.05^{D2}
CT-HF5	0.4 ± 0.06^{AB2}	2.4 ± 0.11^{BC2}
CT-HF5 + N	0.3 ± 0.04^{BC2}	2.5 ± 0.02^{B2}
CT-HF9	0.4 ± 0.01^{A2}	2.3 ± 0.05^{CD3}
CT-HF9 + N	0.3 ± 0.04^{C2}	2.6 ± 0.03^{A1}
CT-SEP	0.3 ± 0.03^{BC3}	4. ± 0.09^{B1}

Note: Different superscript letters indicate significant statistical differences between the surface treatments within same material, different superscript numbers indicate significant statistical differences between materials within the same surface treatment (p ≤ 0.05).

3.1.2. Light transmittance measurements

Table 4 reports direct light transmittance (T%) and absorbance (Abs %) values of the ceramic materials following different surface treatments. Two-way ANOVA revealed a significant effect of material type, surface treatment and their interaction on their light transmission properties ($p < 0.001$). Highest light transmission was demonstrated in VS ceramics in comparison to other lithium silicate based ceramics. Untreated ceramic specimens permitted higher light transmission in comparison to ceramics with treated surfaces. Neutralized specimens permitted less light transmission compared to non-neutralized specimens etched with the same HF etchant concentration. Additionally, light absorption differed among different ceramic materials with greater light absorption seen in the treated specimens in comparison to the control groups. Fig. S2 illustrates the direct light transmission and absorption spectra of the CD ceramic specimens exposed to different surface treatments. It was visually evident that the direct transmission increased with the increasing wavelengths, which was in agreement with the Rayleigh scattering equation stating that higher scattering happens at lower wavelengths.

3.2. Topographical properties

3.2.1. Roughness

Results for roughness parameters *Sa* and *Sq* are reported in Table 5. Two-way ANOVA reported a significant effect of the ceramic type, etching treatment and their interaction on both roughness parameters ($p < 0.05$). Lithium disilicate and zirconia-reinforced lithium silicate ceramics displayed higher roughness (*Sa*) when etched with HF 9% (EC= 2.21 ± 0.14 μm, VS= 1.44 ± 0.16 μm, CD= 3.32 ± 0.2 μm), while lithium aluminium disilicate ceramics displayed higher roughness (*Sa*) when etched with HF 5% (CT= 2.92 ± 0.52 μm). In the specimens etched with the same HF concentration, neutralization postetching decreased the roughness (*Sq*) with both 5% ($p = 0.073$) and 9%

concentrations ($p = 0.023$). Furthermore, the self-etch primer significantly reduced *Sq* ($p < 0.001$ in comparison to the other treatment protocols irrespective of the ceramic type. Fig. 2 demonstrates

Table 5

Topographical characterisation by roughness parameters (Sa and Sq) and wettability (θ˚) of CAD/CAM lithium silicate-based ceramics.

Group	Sa (μm) Mean ± SD	Sq (μm) Mean ± SD	Contact angle (θ˚) Mean ± SD
EC-Control	0.12 ± 0.03^{D12}	0.14 ± 0.04^{D1}	53.9 ± 3.0^{B2}
EC-HF5	0.46 ± 0.11^{C3}	0.54 ± 0.11^{C3}	23.6 ± 2.8^{D1}
EC-HF5 + N	0.52 ± 0.03^{C2}	0.63 ± 0.09^{C2}	35.6 ± 2.3^{C1}
EC-HF9	2.25 ± 0.14^{A2}	2.46 ± 0.13^{A2}	15.8 ± 2.4^{E2}
EC-HF9 + N	1.21 ± 0.27^{B2}	1.34 ± 0.05^{B2}	31.9 ± 1.9^{C1}
EC-SEP	0.17 ± 0.02^{D2}	0.16 ± 0.01^{D23}	91.2 ± 6.4^{A1}
VS-Control	0.16 ± 0.03^{D1}	0.17 ± 0.03^{E1}	44.6 ± 1.3^{B3}
VS-HF5	1.35 ± 0.02^{B2}	1.40 ± 0.02^{B2}	12.4 ± 3.3^{E3}
VS-HF5 + N	0.24 ± 0.01^{C2}	0.35 ± 0.03^{D2}	38.8 ± 1.4^{C1}
VS-HF9	1.45 ± 0.16^{A3}	1.67 ± 0.07^{A3}	15.9 ± 2.3^{E2}
VS-HF9 + N	0.28 ± 0.03^{C3}	0.51 ± 0.06^{C3}	21.5 ± 2.5^{D2}
VS-SEP	0.13 ± 0.04^{D2}	0.14 ± 0.02^{E3}	78.6 ± 2.9^{A2}
CD-Control	0.11 ± 0.01^{C2}	0.13 ± 0.02^{D1}	39.4 ± 2.4^{B3}
CD-HF5	0.77 ± 0.18^{B3}	0.94 ± 0.21^{C23}	18.3 ± 1.7^{E2}
CD-HF5 + N	0.29 ± 0.02^{C2}	0.38 ± 0.04^{D2}	25.0 ± 3.5^{D2}
CD-HF9	3.34 ± 0.20^{A1}	3.27 ± 0.37^{A1}	14.9 ± 1.9^{E2}
CD-HF9 + N	2.85 ± 0.42^{A1}	2.84 ± 0.31^{B1}	33.0 ± 1.1^{C1}
CD-SEP	0.11 ± 0.01^{C2}	0.18 ± 0.02^{D2}	76.3 ± 4.4^{A2}
CT-Control	0.13 ± 0.01^{D12}	0.12 ± 0.02^{D1}	62.4 ± 4.6^{B1}
CT-HF5	2.92 ± 0.52^{A1}	3.01 ± 0.53^{A1}	18.7 ± 1.5^{D2}
CT-HF5 + N	1.87 ± 0.33^{B1}	1.94 ± 0.34^{B1}	19.7 ± 2.2^{D3}
CT-HF9	0.82 ± 0.36^{C4}	0.76 ± 0.36^{C4}	19.9 ± 1.8^{D1}
CT-HF9 + N	0.56 ± 0.11^{CD3}	0.57 ± 0.11^{CD3}	34.7 ± 3.2^{C1}
CT-SEP	0.28 ± 0.06^{CD1}	0.39 ± 0.02^{CD1}	75.6 ± 3.8^{A2}

Note: Different superscript letters indicate significant statistical differences between the surface treatments within the same material, different superscript numbers indicate significant statistical differences between materials within the same surface treatment (p ≤ 0.05).
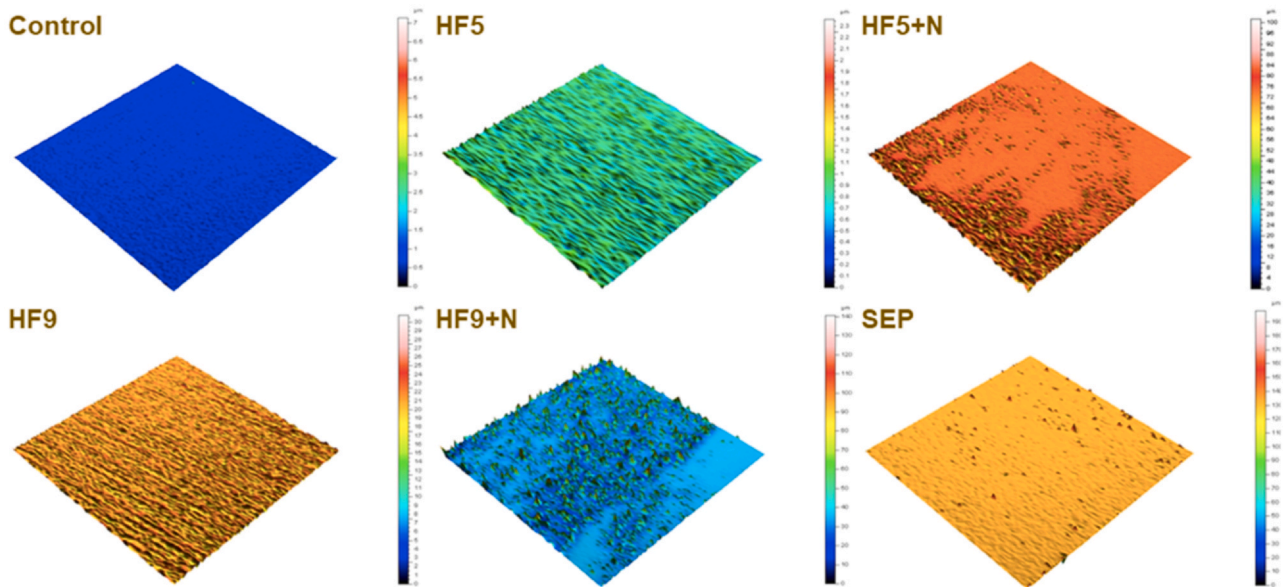
Fig. 2. Representative 3D Topographical maps (2.5 × 2.5 mm²) of ceramic specimens (CEREC Tessera, Dentsply, Sirona) following different surface treatments.

topographical maps of a ceramic specimen (CT) following different surface treatments.

3.2.2. Wettability

Results for the contact angles (θ°) are presented in Table 5 and graphically illustrated in Fig. S3. Two-way ANOVA reported a significant effect of the factors ceramic type, etching treatment and their interaction on the contact angle values ($p < 0.001$). Irrespective of the type of ceramic material, the specimens that were etched with HF (5% and 9%) demonstrated higher wettability than other treatment methods ($p < 0.001$), however, the difference between the wettability of both etchant concentrations was insignificant ($p = 0.977$). Neutralization of the ceramic surfaces decreased their wettability significantly in comparison to ceramics that were etched without subsequent neutralizing treatment ($p < 0.001$). Additionally, the treatment with SEP significantly decreased the wettability of all the LSC's in comparison to the other surface treatments ($p < 0.001$). All treated subgroups were classified as hydrophilic surfaces except for the EC-SEP subgroup that was classified as hydrophobic (θ° = 91.2°). A significant negative correlation between roughness of the ceramics and their contact angle values was found ($r = -0.45$, $p < 0.001$). Fig. S4 presents examples of silane droplets employed for wettability determination of ceramic specimens (CT) following various surface treatments.

3.2.3. Surface microscopy

Representative FE-SEM microscope images of the treated ceramic surfaces are shown in Fig. 3 and Fig. 4. Treated surfaces became increasingly porous and irregular as the etchant concentration increased. Furthermore, neutralized surfaces displayed similar etching patterns to non-neutralized surfaces while ceramics treated with SEP displayed minimal topographical changes compared to those treated with HF.

3.3. Biaxial flexural strength

Table 6 presents the results for B3B biaxial flexural strength testing. Two-way ANOVA showed a strong significant effect of ceramic material and type of surface treatment on σ and F_{max} ($p < 0.001$). However, the interaction between both the variables showed weaker significance on σ ($p = 0.024$) and F_{max} ($p = 0.011$). σ and F_{max} ranged from 225.1 MPa to 421.2 MPa and from 316.0 N to 585.9 N, respectively. Irrespective of the surface treatment to which the ceramic materials were exposed, the σ was observed in the following *descending* order: EC < VS < CD

< CT. Observing the surface treatments, σ was observed in the following *ascending* order: HF9 +N < HF9 < HF5 +N < HF5 < SEP < Control regardless of the type of ceramic material investigated. Significant negative correlations were exhibited between the LSC's roughness parameter *Sq* and their biaxial flexural strength ($r = -0.228$, $p = 0.012$) and fracture load ($r = -0.491$, $p < 0.001$). Fig. S5 illustrates Weibull probability plots for each ceramic materials following different surface treatments. Flexural strength data for surface treatment groups fitted properly in the Weibull distribution model. The characteristic strength ($σ_0$) was highest in the EC Control group ($σ_0 = 614.1$ MPa) and lowest in CD-HF9 +N group ($σ_0 = 336.9$ MPa).

4. Discussion

4.1. General observation

Results from the present study demonstrated that the four CAD/CAM reinforced lithium disilicate glass ceramics were significantly different in their optical, topographical and mechanical properties as well as their effect on the output of a light curing unit. Additionally, all measured properties were significantly affected by the surface treatments to which the ceramic specimens were subjected. Hence, all null hypotheses were rejected.

When formulating an ideal surface treatment regimen for the ceramic restorations, the need to achieve the optimum retentive features should not interfere with the optical and mechanical properties [38]. Literature evidence has confirmed the use of HF as an effective method to promote the bond strength of luting cements to glass ceramic restorations. Manufacturers' recommendations of the investigated LSC's varied regarding etching time (20 s for EC and 30 s for VS, CD, CT), and etchant concentration (5% HF for VS, CT and either 5% or 9% HF for EC, CD) [39–42]. Hence, in the present study, both HF concentrations were examined and the duration was standardized at 30 s. Irrespective of its concentration, HF has been reported to readily penetrate skin causing burns and necrosis of the underlying tissue mucosa and bones [8,10]. The toxicity of HF has led to the exploration of alternative etching agents with weaker acidic potential such as self-etching ceramic primers which have a higher pH (pH = 3.8) in comparison to HF (pH = 2.0) [43]. The addition of a neutralizing step subsequent to the HF etching protocol has been reported to halt the acidic action of HF within the ceramic surface[44]. While some studies have confirmed long-term clinical survival in neutralized etched ceramic surfaces [45], others
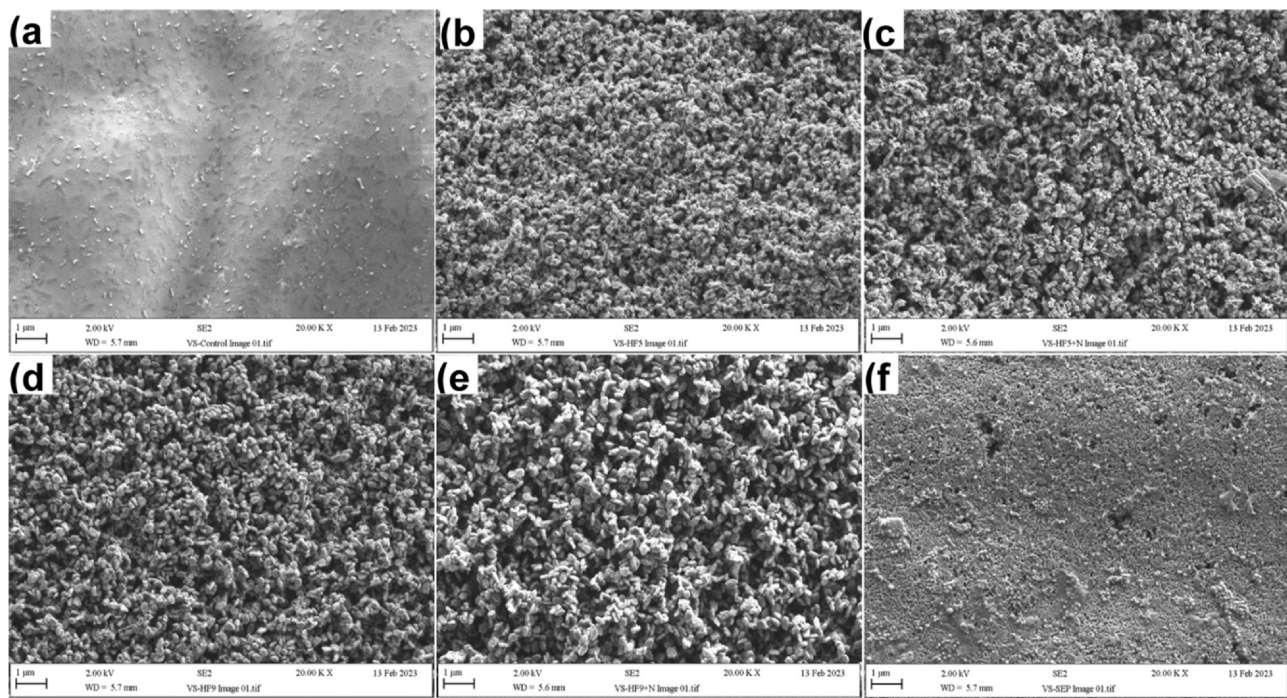
Fig. 3. FE-SEM images (×20,000) exhibiting the surface topography of VS (Vita Suprinity, Vita-Zahnfabrik) following different surface treatments (a) Control, (b) HF5, (c) HF5 +N (d) HF9, (e) HF9 +N and (f) SEP.
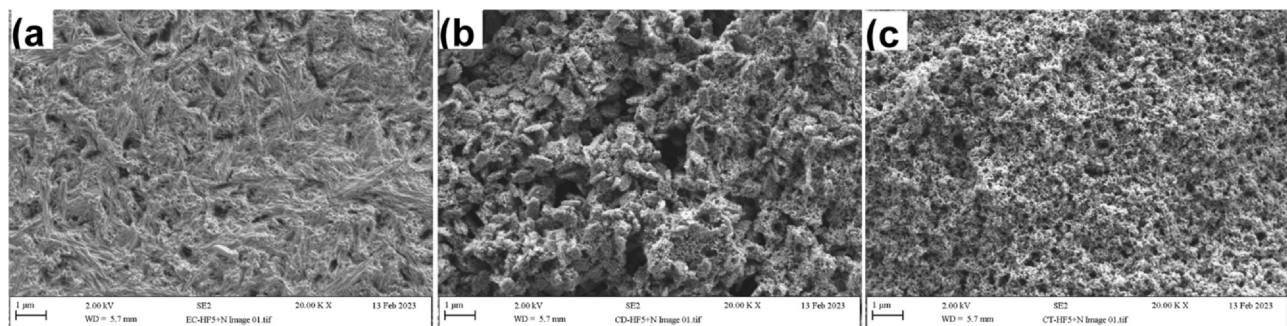
Fig. 4. FE-SEM images (×20,000) exhibiting the surface topography of (a) EC (Ivoclar Vivadent), (b) CD (Dentsply Sirona) and (c) CT (Dentsply Sirona) following the same HF5 +N surface treatment protocol.

claim that the resultant salt precipitation from the neutralizing solution hinders the bonding mechanism leading to suboptimal bond strengths [20]. Therefore, ultrasonic cleaning is an indispensable pre-bonding step to remove residual silicate salts and organic debris that may arise on the internal ceramic surfaces post-etching [46].

Considering that surface treatment of intaglio ceramic surfaces is inevitable when bonding a ceramic restoration to the tooth substrate, it is of utmost importance to consider the effect of surface treatments when evaluating the diverse properties of CAD/CAM restorations and not merely focusing efforts on studying the ceramic material as a solo entity independent of the surface treatments.

4.2. Photometric properties

4.2.1. Irradiance measurements

The minimum radiant exposure required to initiate the activation of camphorquinone initiated resin cements is 16 J/cm^2, which can be achieved with a LCU emitting 400 or 800 mW/cm^2 in a 40 or 20 s exposure interval, respectively [47]. Upon interposition with a ceramic substrate, the attenuation of a LCU's output is directly proportional to the thickness and crystalline density of the ceramic material [48].

In this study, lithium disilicate ceramics (EC) showed significantly greater transmitted light output in comparison to the zirconia reinforced lithium silicates and lithium aluminium disilicates, with the power, radiant exposure and irradiance of the LCU ranging from 78.4 to 85.4 mW, 11.7–13.3 J/cm^2 and 577.2–634.4 mW/cm^2, respectively within the 20 s light exposure period. This observation is in agreement with other studies in the literature [48,49], and could be rationalised as a result of differences in the crystal size and chemical composition. In EC specimens, the lithium disilicate crystal sizes range between 1.0 and 1.5 μm which are larger than those found in VS and CD zirconia reinforced lithium silicates (0.5–0.7 μm) and CT lithium aluminium disilicates (0.2–0.3 μm). The disperse interlocking of crystals in the EC permits less scattering of light and thus greater transmittance in comparison to the other LCS's with densely intermeshed crystalline networks. The degree of LCU light attenuation in terms of power (mW), irradiance (mW/cm^2) and radiant exposure (J/cm^2) differed significantly among the CAD/CAM LSC's and within different surface treatments. The greatest percentage of loss of LCU's output (up to 84% power loss) was demonstrated upon interposition with the CT specimens, which could be explained by the additional virgilite crystals found in the crystalline microstructure of CT leading to a greater light

Table 6

Biaxial flexural strength (MPa), fracture load (N), characteristic strength (MPa), Weibull modulus (m) and coefficient of determination (R^2) of CAD/CAM lithium silicate-based ceramics by B3B method.

Group	Biaxial flexural strength σ (MPa) Mean ± SD	Fracture load F_{max} (N) Mean ± SD	Characteristic strength $σ_0$ (MPa) [95% CI]	Weibull modulus (m) [95% CI]	Coefficient of determination (R^2)
EC-Control	421.2 ± 57.0[A1]	585.9 ± 71.7[A1]	614.1 [658.9–573.3]	9.4 [12.7–5.2]	0.967
EC-HF5	382.8 ± 64.9[A1]	529.2 ± 88.1[A1]	556.8 [611.3–508.6]	7.1 [9.6–3.9]	0.978
EC-HF5 + N	376.2 ± 70.9[A1]	528.9 ± 101.3[A1]	572.5 [641.0–513.1]	5.9 [7.9–3.2]	0.986
EC-HF9	366.0 ± 63.6[A1]	516.2 ± 82.3[A1]	550.0 [604.9–501.5]	6.9 [9.4–3.8]	0.942
EC-HF9 + N	360.3 ± 87.4[A1]	505.3 ± 123.9[A1]	550.0 [629.9–482.2]	4.9 [6.6–2.7]	0.943
EC-SEP	384.4 ± 62.3[A1]	547.5 ± 104.9[A1]	589.9 [657.1–531.3]	6.2 [8.3–3.4]	0.962
VS-Control	379.0 ± 49.9[A1]	530.4 ± 75.9[A1]	561.2 [608.9–518.5]	8.2 [11.0–4.5]	0.972
VS-HF5	354.3 ± 52.4[AB1]	513.2 ± 74.9[A1]	544.6 [591.4–502.7]	8.1 [10.9–4.4]	0.945
VS-HF5 + N	330.2 ± 46.2[ABC12]	475.9 ± 53.2[AB1]	497.7 [530.6–467.7]	10.4 [14.0–5.7]	0.932
VS-HF9	314.2 ± 51.2[BC12]	444.4 ± 75.2[AB12]	473.4 [520.6–431.7]	6.9 [9.4–3.8]	0.917
VS-HF9 + N	287.4 ± 59.2[C12]	416.9 ± 98.2[B12]	454.9 [522.1–398.0]	4.8 [6.5–2.6]	0.950
VS-SEP	357.8 ± 26.1[AB1]	520.9 ± 41.4[A1]	539.2 [563.8–516.3]	14.9 [20.1–8.2]	0.966
CD-Control	401.2 ± 40.0[A1]	559.4 ± 48.4[A1]	578.2 [607.6–551.0]	13.4 [18.1–7.4]	0.940
CD-HF5	281.9 ± 62.3[BC2]	398.0 ± 74.4[BC2]	411.6 [457.7–371.3]	6.3 [8.4–3.4]	0.967
CD-HF5 + N	272.8 ± 38.9[BC2]	367.4 ± 56.7[C2]	391.6 [427.0–359.8]	7.6 [10.3–4.2]	0.825
CD-HF9	253.4 ± 50.8[C2]	365.2 ± 79.9[C2]	395.4 [450.4–348.5]	5.1 [6.9–2.8]	0.920
CD-HF9 + N	225.1 ± 31.9[C2]	316.0 ± 51.6[C2]	336.9 [370.2–307.4]	7.0 [9.5–3.8]	0.954
CD-SEP	331.71 ± 39.9[B12]	467.7 ± 67.9[B12]	492.7 [535.2–454.6]	8.0 [10.8–4.4]	0.979
CT-Control	284.5 ± 54.8[A2]	386.5 ± 77.0[A2]	415.7 [466.7–371.6]	5.8 [7.7–3.1]	0.948
CT-HF5	277.2 ± 29.2[A2]	379.5 ± 43.2[A2]	399.4 [426.6–374.7]	10.1 [13.6–5.5]	0.945
CT-HF5 + N	273.3 ± 40.6[A2]	383.0 ± 61.9[A2]	407.5 [447.6–372.0]	7.1 [9.5–3.9]	0.945
CT-HF9	269.9 ± 49.7[A2]	379.6 ± 73.8[A2]	411.6 [461.9–368.0]	5.8 [7.8–3.1]	0.957
CT-HF9 + N	253.3 ± 80.9[A2]	355.8 ± 98.1[A2]	391.4 [458.2–336.1]	4.2 [5.7–2.3]	0.948
CT-SEP	283.3 ± 68.2[A2]	384.4 ± 96.6[A2]	419.9 [485.6–364.7]	4.6 [6.1–2.5]	0.873

Note: Different superscript letters indicate significant statistical differences between the surface treatments within same material, different superscript numbers indicate significant statistical differences between materials within the same surface treatment ($p \leq 0.05$).

absorption and decreased transmission [5]. The difference in the LCU's output between the control and etched specimens could be explained by the presences of insoluble silica fluoride salts that form in the latter interfering with the degree of light transmitted [50]. Irrespective of the presence of a neutralizing post-etching step, the investigated LSC's reduced the LCU's radiant exposure below the obligated threshold ($< 16 \, J/cm^2$) [47]. Hence, this indicates the need for longer curing times (40 s) when using light-cured resin cements or the substitution with dual cured resin cement alternatives.

4.2.2. Light transmittance measurements

Translucency of ceramics can be measured using one of three main methods: Direct light transmission, total light transmission (direct + diffuse light), and spectral reflectance (e.g. translucency parameter and contrast ratio). Translucency of glass ceramics is affected by their crystalline structure, grain size, degree of pigmentation in addition to the quantity and size of surface defects and porosities [35,51]. When the crystal size is less than the visible light wavelength (350–800 nm), the glass ceramic will acquire a transparent appearance [52]. Absorbance (Abs%) is an indicator of the colorants present in the glass ceramics, hence the higher chromophores available in the ceramic, the higher absorbance it will exhibit [34]. The UV-Vis Spectrometer device is frequently employed in the literature to measure the direct light transmittance (T%) of dental ceramics and mean T% and Abs% are most commonly reported at the 525 nm wavelength [35,53].

T% was found highest in the VS ceramic specimens for all surface treatment groups in comparison to the remaining LSC's. Available literature supports this finding, stating that higher translucency and light transmission was exhibited in zirconia-reinforced lithium silicates than in lithium disilicate glass ceramics [52,54]. This outcome has been

justified by the needle-like crystal microstructure found in zirconia-reinforced lithium silicates allowing for increased glass content in the surrounding matrix [55]. Neutralized ceramic specimens displayed less T% than their non-neutralized counterparts, which could be explained by the presence of fluorosilicate precipitates of Na and Ca in the former. Greater apparent light absorption (Abs%) was found in LSC's post-surface treatment than in non-treated ceramics, this could be due to the changes in the surface micromorphology which altered the pathway of light passage and degree of light absorption [56]. Highest Abs% was seen in the EC specimens etched with HF9 (2.8%) and CD specimens etched with HF5 (2.7%), while the least Abs% was seen in the VS treated with SEP (1.7%). A previous study examined the effect of HF etching, airborne particle abrasion and laser treatment on the optical properties and colour stability of ceramic veneers and concluded significant changes in the tristimulus optical measurements of veneers post-treatment especially in the specimens with decreased (< 1.0 mm) thicknesses [28]. To eliminate any bias from the effect of ceramic shade and/or translucency level on the measured properties, all investigated ceramics in the current study were sectioned from high translucent (HT) blocks in shade A2 with uniform thickness (1.5 mm). A wavelength dependence in both T% and Abs% properties of the LSC's, with higher transmission and lower absorption evident within higher wavelength bands was found. This could imply cementing LSC restorations with resin luting agents that require photoactivation of shorter wavelength-activated photo-initiators [56,57]. Despite the neutralization process in the current study, all neutralized LCS's exhibited sufficient levels of translucency, allowing them to be employed where there is an aesthetic demand.

4.3. Topographical properties

4.3.1. Roughness

Different HF etching regimens have been studied in the literature with the etching duration as the most common experimental factor [15, 26, 58]. Moreover, effects of the temperature and concentration of ceramic acid etchants have been explored [59–61]. In the present study, irrespective of the executed etching protocol, HF resulted in significant topographical alterations seen in the form of nanoporosities, striations and grooves within the etched intaglio ceramic surface (Fig. 2). Etching with 9% HF concentration promoted greater roughness (Sa, Sq) in the EC, VS and CD ceramic specimens in comparison to 5% concentration, which has also been reported in previous studies [62,63]. On the other hand, Prochnow et al. reported comparable roughness in ceramics when etched with different HF concentrations [59]. This could be explained by the difference in profilometry methods employed for measurement (contact versus noncontact) or different roughness parameters measured (two-dimensional versus three-dimensional). The addition of a neutralization step post-etching altered the roughness of the LSC's as was demonstrated in the topographical surface maps (Fig. 2) and microscopic images (Figs. 3, 4) in the form of inconsistent peaks and valleys interrupted by smooth areas that could exemplify any residual NaF or CaF_2 salts persisting within the ceramic surface after ultrasonic cleaning. Furthermore, LSC's treated with self-etch primer presented the lowest roughness among all the surface treated groups. This observation has been supported by multiple studies in the literature [63–65] and could be explained by the adsorption of the silane by the preconditioned ceramic surfaces combined with the weak acidic capability of the tetrabutyl ammonium hydrogen difluoride. In general, neutralizing the LSC's improved their roughness, and resulted in surfaces with higher micromechanical retentive features necessary for bonding to the tooth substrate.

4.3.2. Wettability

The efficacy of the surface treatments was also evaluated by investigating the degree of hydrophilicity of the CAD/CAM LSC substrates by means of contact angle measurements (θ°). The sessile drop profile

analysis was chosen in this present study due to its technical convenience and wide popularity in the literature [26, 66, 67]. In the present study, HF etching enhanced the wettability of LSC's regardless of the etchant concentration or the presence of a subsequent neutralizing step. Ceramic surfaces that were etched with HF exhibited the lowest contact angles ranging from 12.4° (VS-HF5) to 23.6° (EC-HF5), while the surfaces that were neutralized post-etching displayed slightly higher contact angles ranging from 19.7° (CT-HF5 + N) to 38.8° (VS-HF5 + N). This can be rationalised by the HF's removal of low surface energy contaminants and organic debris hence increasing the density of hydroxyl groups and creating a high energy ceramic surface that is readily wet by the silane primer [68]. Coating with the SEP significantly reduced the wettability of all LSC surfaces in this study (Fig. S4.b), to the extent that rendered the EC ceramics as hydrophobic surfaces. This finding corresponds with previous studies [43,69] and has been explained by the chemically bonded film found on the SEP treated surfaces formed between the trimethoxypropyl methaycrylate in SEP and the silanol (Si-OH) found within the ceramic surfaces, which reduces the LSC's surface energy and subsequent wettability.

4.4. Biaxial flexural strength

The ball-on-three-balls (B3B) test has validated its tolerance to minor specimen inaccuracies such as flatness and alignment deviations in contrast to the traditional rotationally symmetrical biaxial testing configurations, hence proving the B3B to be an instrumental testing method to measure the biaxial flexural strength of brittle ceramics with smaller dimensions [29,70]. In this study, square ceramic plates (12 × 12 mm^2) were employed in the B3B testing apparatus instead of the conventional disc configuration to accommodate the fixed geometry of CAD/CAM blocks, based on evidence in the literature stating no differences were found in the biaxial flexural strength results between both geometries [31,71]. The ceramic specimens were positioned with the treated surfaces facing towards the tensile forces and away from the compressive loading component in order to simulate the clinical intraoral scenarios in which the intaglio ceramic restorations undergo tensile forces opposing the compressive occlusal loads. The minimum required threshold of flexural strength of ceramic materials varies according to the clinically indicated dental restoration; ranging as low as 50 MPa for adhesively cemented monolithic single-unit anterior restorations, to 800 MPa needed in a four-unit prosthesis [72]. Based on the flexural strength findings in the present study, all the investigated LSC's displayed adequate strength to be employed for single-unit restorations in the anterior region, except for the EC specimens which displayed higher strength (> 350 MPa) expanding their clinical indications to the three-unit prosthesis extending to the premolar region.

Results of the biaxial flexural strength of EC, VS and CD control groups were found within the range previously reported for B3B tests performed in the literature [31, 73, 74]. To date, CT is the most recently introduced LSC, and we could not find any studies reporting biaxial flexural strength for this CAD/CAM ceramic by means of the B3B testing method. The manufacturers of CT claim that it offers biaxial flexural strength > 700 MPa, which is significantly higher than that found in the current study (253.3 − 284.5 MPa). A study by Demirel et al. investigating the effect of different glazing methods on the biaxial flexural strength of the CT, reported higher strength (374.2–463.2 MPa) than that found in the current study [75]. The reported increased biaxial flexural strength results could be attributed to the difference in testing method (piston-on-three balls) or due to the presence of an additional glaze firing treatment which did not take place in the present study.

Etching with HF significantly reduced the biaxial flexural strength of all the investigated LSC's with both etchant concentrations and whether neutralization took place or not. This outcome has been reported previously in the literature [58,76] and is explained by the increased surface irregularities that are created by the etching process that act as

stress concentration areas at which cracks initiate and propagate upon load application, hence weakening the glass ceramic. Lima et al. compared the effect of different surface treatments on the biaxial flexural strength of EC, VS and CD and observed similar outcomes as the present study with higher reported strength in the former [77]. This could be explained by the dissimilar testing methodology as well as the performance of silane coating treatment.

Neutralizing the etched LSC specimens slightly decreased the biaxial flexural strength, however this decrease was not statistically significant ($p > 0.05$) hence justifying neutralization as an important addition to the pre-cementation regimen of LSC's. Moreover, the SEP groups exhibited higher flexural strength than the other surface treated groups, which has been supported by evidence reported in the literature [77,78] and explained by the decreased etching potential of the SEP as previously confirmed in the topographical segment of this present study.

In the present study Weibull modulus and characteristic strength were obtained from the linear regression analysis which demonstrated that the data set of 10 LSC specimens per subgroup adequately aligned within the linear model as proven by their high coefficient of determination ($0.82 < R^2 < 0.98$) hence allowing us to infer that the dispersion of strength values within each subgroup can be generalized to a larger population. Evidence in the literature has stated that although it is preferable to perform Weibull analysis on 30 specimens, it has also been confirmed that estimates of characteristic strength can be converted to population values when ten or more specimens are used [79]. Irrespective of the surface treatment protocol, the EC ceramic materials displayed the highest mean σ_0 (572.5 MPa) while the CT specimens exhibited the lowest mean σ_0 (407.5 MPa). Irrespective of the type of ceramic material, the surface treatment that yielded the highest mean σ_0 was SEP (510.43 MPa) and HF9 + N yielded the lowest mean σ_0 (433.3 MPa). Based on Weibull modulus, higher reliability of strength was found in the VS-SEP and CD-Control groups (m = 14.9 and 13.4, respectively) while the least reliability was exhibited in the CT-SEP and CT-HF9 + N groups (m = 4.6 and 4.2, respectively). Both σ_0 and m in the present studies fell within the range of values for the LSC's previously observed in the literature [31,77].

Based on the findings of this study, neutralizing lithium silicate-based glass ceramics was not detrimental to their flexural strength nor surface properties. Hence, clinicians should consider the application of a neutralizing agent post HF etching as an effective and safe pre-cementation protocol when lithium silicate-based ceramic restorations are indicated.

5. Conclusions

Within the limitations of this study, the following conclusions can be derived:

1. All investigated LSC's significantly reduced the output from the LCU, the decline was material dependent while the effect of surface treatment was insignificant.
2. Neutralized LSC's exhibited satisfactory degrees of light transmission, while higher light transmission was exhibited in the untreated ceramic specimens.
3. Neutralization post-etching incited favourable topographical alterations necessary for bonding LSC's dental restorations, whereas the self-etching primer decreased the roughness and wettability significantly.
4. Biaxial flexural strength was reduced for all LSC's after post-treatment, emphasizing the importance of adhesive cementation of the LSC dental restorations.
5. Post-etching neutralization is a promising treatment method for safe surface alterations of the intaglio surfaces in LSC dental restorations.

Appendix A. Supporting information

Supplementary data associated with this article can be found in the online version at doi:10.1016/j.dental.2023.07.004.

References

[1] Holand W., Beall G.H. Glass-ceramic technology: John Wiley & Sons; 2019.
[2] Lubauer J, Belli R, Peterlik H, Hurle K, Lohbauer U. Grasping the Lithium hype: insights into modern dental Lithium Silicate glass-ceramics. Dent Mater 2022;38(2). 318-32.
[3] Rauch A, Reich S, Dalchau L, Schierz O. Clinical survival of chair-side generated monolithic lithium disilicate crowns: 10-year results. Clin Oral Investig 2018;22(4):1763–9.
[4] Willard A, Chu T-MG. The science and application of IPS e. Max dental ceramic. Kaohsiung J Med Sci 2018;34(4). 238-42.
[5] Phark JH, Duarte Jr S. Microstructural considerations for novel lithium disilicate glass ceramics: a review. J Esthet Restor Dent 2022;34(1):92–103.
[6] Marchesi G, Camurri Piloni A, Nicolin V, Turco G, Di Lenarda R. Chairside CAD/CAM materials: current trends of clinical uses. Biology 2021;10(11):1170.
[7] Huang S, Li Y, Wei S, Huang Z, Gao W, Cao P. A novel high-strength lithium disilicate glass-ceramic featuring a highly intertwined microstructure. J Eur Ceram Soc 2017;37(3). 1083-94.
[8] Bajraktarova-Valjakova E., Grozdanov A., Guguvcevski L., Korunoska-Stevkovska V., Kapusevska B., Gigovski N., et al. Acid etching as surface treatment method for luting of glass-ceramic restorations, part 1: acids, application protocol and etching effectiveness. Open access Macedonian journal of medical sciences. 2018;6(3):568.
[9] Borges GA, Sophr AM, De Goes MF, Sobrinho LC, Chan DC. Effect of etching and airborne particle abrasion on the microstructure of different dental ceramics. J Prosthet Dent 2003;89(5):479–88.
[10] Ho GW, Matinlinna JP. Insights on ceramics as dental materials. Part II: chemical surface treatments. Silicon 2011;3(3). 117-23.
[11] Oliveira-Ogliari A, Vasconcelos CS, Bruschi RC, Gonçalves AP, Ogliari FA, Moraes RR. Thermal silicatization: a new approach for bonding to zirconia ceramics. Int J Adhes Adhes 2014;48:164–7.
[12] Della Bona A. Bonding to ceramics: scientific evidences for clinical dentistry: Artes Médicas; 2009.
[13] Ozcan M, Allahbeickaraghi A, Dündar M. Possible hazardous effects of hydrofluoric acid and recommendations for treatment approach: a review. Clin Oral Invest 2012;16(1):15–23.
[14] Canay S, Hersek N, Ertan A. Effect of different acid treatments on a porcelain surface. J Oral Rehabil 2001;28(1):95–101.
[15] Leite FP, Özcan M, Valandro LF, Cunha Moreira CH, Amaral R, Bottino MA, et al. Effect of the etching duration and ultrasonic cleaning on microtensile bond strength between feldspathic ceramic and resin cement. J Adhes 2013;89(3). 159-73.
[16] Sriamporn T, Kraisintu P, See LP, Swasdison S, Klaisiri A, Thamrongananskul N. Effect of different neutralizing agents on feldspathic porcelain etched by hydrofluoric acid. Eur J Dent 2019;13(1):75–81.
[17] Panah FG, Rezai SM, Ahmadian L. The influence of ceramic surface treatments on the micro-shear bond strength of composite resin to IPS Empress 2. J Prosthodont 2008;17(5):409–14.
[18] Wang X, Zhang Y, Ni L, You C, Ye C, Jiang R, et al. A review of treatment strategies for hydrofluoric acid burns: current status and future prospects. Burns 2014;40(8):1447–57.
[19] Özcan M, Volpato C. Surface conditioning protocol for the adhesion of resin-based materials to glassy matrix ceramics: how to condition and why. J Adhes Dent 2015;17(3):292–3.
[20] Saavedra G, Ariki EK, Federico CD, Galhano G, Zamboni S, Baldissara P, et al. Effect of acid neutralization and mechanical cycling on the microtensile bond strength of glass-ceramic inlays. Oper Dent 2009;34(2):211–6.
[21] Bottino M, Snellaert A, Bergoli C, Özcan M, Bottino M, Valandro L. Effect of ceramic etching protocols on resin bond strength to a feldspar ceramic. Oper Dent 2015;40(2). E40-E6.
[22] Lopes GC, Perdigão J, Baptista D, Ballarin A. Does a self-etching ceramic primer improve bonding to lithium disilicate ceramics? Bond strengths and FESEM analyses. Oper Dent 2019;44(2):210–8.
[23] Tribst JP, Diamantino PJ, de Freitas MR, Tanaka IV, Silva-Concílio LR, de Melo RM, et al. Effect of active application of self-etching ceramic primer on the long-term bond strength of different dental CAD/CAM materials. J Clin Exp Dent 2021;13(11). e1089-e95.
[24] Queiroz-Lima G, Strazzi-Sahyon HB, Maluly-Proni AT, Fagundes TC, Briso ALF, Assunção WG, et al. Surface characterization of indirect restorative materials submitted to different etching protocols. J Dent 2022:104348.

[25] Preoteasa C., Sultan A.N., Popa L., Ionescu E., Iosif L., Ghica M., et al. Wettability of some dental materials. Optoelectronics and Advanced Materials-Rapid Communications. 2011;5(August 2011):874–8.

[26] Ramakrishnaiah R, Alkheraif AA, Divakar DD, Matinlinna JP, Vallittu PK. The effect of hydrofluoric acid etching duration on the surface micromorphology, roughness, and wettability of dental ceramics. Int J Mol Sci 2016;17(6):822.

[27] Villarroel M, Fahl N, De Sousa AM, De, Oliveira Jr. OB. Direct esthetic restorations based on translucency and opacity of composite resins. J Esthet Restor Dent 2011;23(2):73–87.

[28] Turgut S, Bağış B, Korkmaz FM, Tamam E. Do surface treatments affect the optical properties of ceramic veneers? The. J Prosthet Dent 2014;112(3):618–24.

[29] Börger A, Supancic P, Danzer R. The ball on three balls test for strength testing of brittle discs: stress distribution in the disc. J Eur Ceram Soc 2002;22(9–10). 1425-36.

[30] Rasche S, Strobl S, Kuna M, Bermejo R, Lube T. Determination of strength and fracture toughness of small ceramic discs using the small punch test and the ball-on-three-balls test. Procedia Mater Sci 2014;3:961–6.

[31] Wendler M, Belli R, Petschelt A, Mevec D, Harrer W, Lube T, et al. Chairside CAD/CAM materials. Part 2: Flexural strength testing. Dent Mater 2017;33(1):99–109.

[32] Peumans M, Valjakova EB, De Munck J, Mishevska CB, Van Meerbeek B. Bonding effectiveness of luting composites to different CAD/CAM materials. J Adhes Dent 2016;18(4):289–302.

[33] Moura DMD, Araújo AMMd, Souza KBd, Veríssimo AH, Tribst JPM, Souza ROdA. Hydrofluoric acid concentration, time and use of phosphoric acid on the bond strength of feldspathic ceramics. Braz Oral Res 2020:34.

[34] Brodbelt R, O'brien W, Fan P. Translucency of dental porcelains. J Dent Res 1980;59(1):70–5.

[35] Della Bona A, Nogueira AD, Pecho OE. Optical properties of CAD–CAM ceramic systems. J Dent 2014;42(9):1202–9.

[36] Law KY. Definitions for hydrophilicity, hydrophobicity, and superhydrophobicity: getting the basics right. J Phys Chem Lett 2014;5(4):686–8.

[37] 843–5 DE. Advanced technical ceramics-Monolithic ceramics; mechanical tests at room temperature-Part 5: statistical analysis. Dtsch Inst Fur Norm–DIN. 2007.

[38] Venturini AB, Prochnow C, May LG, Bottino MC, Valandro LF. Influence of hydrofluoric acid concentration on the flexural strength of a feldspathic ceramic. J Mech Behav Biomed Mater 2015;48:241–8.

[39] Sirona D. Celtra Duo Technical product information. 2017.

[40] Sirona D. Cerec Tessera. Technical Product Information. 2021.

[41] Zahnfabrik V. VITA ENAMIC Technical and Scientific Documentation. VITA Zahnfabrik: Bad Sackingen, Germany. 2019.

[42] Vivadent I. Scientific Documentation IPS e. max CAD. Liechtenstein. 2011.

[43] Grégoire G, Poulet P-P, Sharrock P, Destruhaut F, Tavernier B. Hydrofluoric acid etching versus self-etching glass ceramic primer: consequences on the interface with resin cements. Oral Health Care 2019;4:1–7.

[44] Özcan M, Vallittu PK. Effect of surface conditioning methods on the bond strength of luting cement to ceramics. Dent Mater 2003;19(8):725–31.

[45] Bresser R, Gerdolle D, van den Heijkant I, Sluiter-Pouwels L, Cune M, Gresnigt M. Up to 12 years clinical evaluation of 197 partial indirect restorations with deep margin elevation in the posterior region. J Dent 2019;91:103227.

[46] Martins ME, Leite FP, Queiroz JR, Vanderlei AD, Reskalla HN, Ozcan M. Does the ultrasonic cleaning medium affect the adhesion of resin cement to feldspathic ceramic. J Adhes Dent 2012;14(6):507–9.

[47] Shen C, Rawls HR, Esquivel-Upshaw JF. Philos' Sci Dent Mater E-Book: Elsevier Health Sci 2021.

[48] Stawarczyk B, Awad D, Ilie N. Blue-light transmittance of esthetic monolithic CAD/CAM materials with respect to their composition, thickness, and curing conditions. Oper Dent 2016;41(5). 531-40.

[49] Aldryhim H, El-Mowafy O, McDermott P, Prakki A. Hardness of resin cements polymerized through glass-ceramic veneers. Dent J 2021;9(8):92.

[50] Maruo Y, Nishigawa G, Irie M, Yoshihara K, Matsumoto T, Minagi S. Does acid etching morphologically and chemically affect lithium disilicate glass ceramic surfaces? J Appl Biomater Funct Mater 2017;15(1):93–100.

[51] Ilie N, Hickel R. Correlation between ceramics translucency and polymerization efficiency through ceramics. Dent Mater 2008;24(7):908–14.

[52] Awad D, Stawarczyk B, Liebermann A, Ilie N. Translucency of esthetic dental restorative CAD/CAM materials and composite resins with respect to thickness and surface roughness. The. J Prosthet Dent 2015;113(6):534–40.

[53] Kaczmarek K., Leniart A., Lapinska B., Skrzypek S., Lukomska-Szymanska M.. Selected Spectroscopic Techniques for Surface Analysis of Dental Materials: A Narrative Review. Materials (Basel). 2021;14(10).

[54] Vichi A, Carrabba M, Paravina R, Ferrari M. Translucency of ceramic materials for CEREC CAD/CAM system. J Esthet Restor Dent 2014;26(4):224–31.

[55] Apel E, van't Hoen C, Rheinberger V, Höland W. Influence of ZrO2 on the crystallization and properties of lithium disilicate glass-ceramics derived from a multi-component system. J Eur Ceram Soc 2007;27(2–3):1571–7.

[56] Pacheco RR, Carvalho AO, André CB, Ayres APA, de Sá RBC, Dias TM, et al. Effect of indirect restorative material and thickness on light transmission at different wavelengths. J Prosthodont Res 2019;63(2):232–8.

[57] Watts D, Cash A. Analysis of optical transmission by 400–500 nm visible light into aesthetic dental biomaterials. J Dent 1994;22(2):112–7.

[58] Zogheib LV, Bona AD, Kimpara ET, Mccabe JF. Effect of hydrofluoric acid etching duration on the roughness and flexural strength of a lithium disilicate-based glass ceramic. Braz Dent J 2011;22:45–50.

[59] Prochnow C, Venturini AB, Grasel R, Bottino MC, Valandro LF. Effect of etching with distinct hydrofluoric acid concentrations on the flexural strength of a lithium disilicate-based glass ceramic. J Biomed Mater Res Part B: Appl Biomater 2017;105(4). 885-91.

[60] Menees TS, Lawson NC, Beck PR, Burgess JO. Influence of particle abrasion or hydrofluoric acid etching on lithium disilicate flexural strength. J Prosthet Dent 2014;112(5):1164–70.

[61] Sundfeld D, Correr-Sobrinho L, Pini NIP, Costa AR, Sundfeld RH, Pfeifer CS, et al. The effect of hydrofluoric acid concentration and heat on the bonding to lithium disilicate glass ceramic. Braz Dent J 2016;27. 727-33.

[62] Donmez MB, Okutan Y, Yucel MT. Effect of prolonged application of single-step self-etching primer and hydrofluoric acid on the surface roughness and shear bond strength of CAD/CAM materials. Eur J Oral Sci 2020;128(6):542–9.

[63] Azevedo VLB, de Castro EF, Bonvent JJ, de Andrade OS, Nascimento FD, Giannini M, et al. Surface treatments on CAD/CAM glass–ceramics: Influence on roughness, topography, and bond strength. J Esthet Restor Dent 2021;33(5). 739-49.

[64] Dimitriadi M, Zinelis S, Zafiropoulou M, Silikas N, Eliades G. Self-etch silane primer: reactivity and bonding with a lithium disilicate ceramic. Materials 2020;13(3):641.

[65] El-Damanhoury HM, Gaintantzopoulou MD. Self-etching ceramic primer versus hydrofluoric acid etching: etching efficacy and bonding performance. J Prosthodont Res 2018;62(1):75–83.

[66] Ramakrishnaiah R, Alkheraif AA, Divakar DD, Alghamdi KF, Matinlinna JP, Lung CYK, et al. The effect of lithium disilicate ceramic surface neutralization on wettability of silane coupling agents and adhesive resin cements. Silicon 2018;10(6):2391–7.

[67] Huhtamäki T, Tian X, Korhonen JT, Ras RHA. Surface-wetting characterization using contact-angle measurements. Nat Protoc 2018;13(7). 1521-38.

[68] Marshall SJ, Bayne SC, Baier R, Tomsia AP, Marshall GW. A review of adhesion science. Dent Mater 2010;26(2). e11-e6.

[69] Sattabanasuk V, Charnchairerk P, Punsukumtana L, Burrow MF. Effects of mechanical and chemical surface treatments on the resin-glass ceramic adhesion properties. J Invest Clin Dent 2017;8(3):e12220.

[70] Nohut S. A general formulation for strength prediction of advanced ceramics by ball-on-three-balls (B3B)-test with different multiaxial failure criteria. Ceram Int 2012;38(3). 2411-20.

[71] Danzer R, Harrer W, Supancic P, Lube T, Wang Z, Börger A. The ball on three balls test—Strength and failure analysis of different materials. J Eur Ceram Soc 2007;27(2–3):1481–5.

[72] Dentistry - Ceramic Materials BS EN ISO 6872:2015+A1:2018. International Organization for Standardization2018. p. 12–3.

[73] Corado HP, da Silveira PH, Ortega VL, Ramos GG, Elias CN. Flexural strength of vitreous ceramics based on lithium disilicate and lithium silicate reinforced with zirconia for CAD/CAM. Int J Biomater 2022:2022.

[74] Soares VO, Serbena FC, Mathias I, Crovace MC, Zanotto ED. New, tough and strong lithium metasilicate dental glass-ceramic. Ceramics International. 2021;47(2). 2793-801.

[75] Demirel M., Diken Türksayar A.A., Donmez M.B.Translucency, color stability, and biaxial flexural strength of advanced lithium disilicate ceramic after coffee thermocycling. J Esthet Restor Dent. 2022.

[76] Xiaoping L, Dongfeng R, Silikas N. Effect of etching time and resin bond on the flexural strength of IPS e. max Press glass ceramic. Dent Mater 2014;30(12). e330-e6.

[77] Lima CM, da Silva NR, Martins JD, Miranda JS, Tanaka R, e, Souza ROdA, et al. Effect of different surface treatments on the biaxial flexure strength, Weibull characteristics, roughness, and surface topography of bonded CAD/CAM silica-based ceramics. Dent Mater 2021;37(3). e151-e61.

[78] Tribst JPM, Dal Piva AMdO, Lopes GC, Borges ALS, Bottino MA, Özcan M, et al. Biaxial flexural strength and Weibull characteristics of adhesively luted hybrid and reinforced CAD/CAM materials to dentin: effect of self-etching ceramic primer versus hydrofluoric acid etching. J Adhes Sci Technol 2020;34(12):1253–68.

[79] Quinn JB, Quinn GD. A practical and systematic review of Weibull statistics for reporting strengths of dental materials. Dent Mater 2010;26(2):135–47.